ECCOMAS Congress 2016
VII European Congress on Computational Methods in Applied Sciences and Engineering
M. Papadrakakis, V. Papadopoulos, G. Stefanou, V. Plevris (eds.)
Crete Island, Greece, 5–10 June 2016

NUMERICAL SIMULATION OF BUOYANT PLUMES USING A FIXED POINT ITERATIVE METHOD

B. Bermúdez[1], A. Rangel-Huerta[1], W. Fermín Guerrero S.[2] and J. D. Alanís [3]

[1] F. C. C. BUAP
14 Sur y San Claudio
Puebla, México
e-mail: bbj@cs.buap.mx, arangel@cs.buap.mx
[2] F. C. F. M. BUAP
18 Sur y San Claudio
Puebla, México
e-mail: wferming@gmail.com
[3] Universidad Tecnológica de Puebla
Carrera de Tecnologías de la Información y Comunicación, UTP
Antiguo Camino a la Resurrección 1002-A Col. Zona Industrial Oriente
Puebla, México
e-mail:david.alanis@utpuebla.edu.mx

Keywords: Buoyant plumes, Boussinesq approximation, Rayleigh number, high convection dominated flows.

Abstract. *A numerical simulation of unsteady plumes for driven thermal high convection dominated flows is presented in this work. The problem is of practical interest for example in the cooling of electronic devices and heat transfer from pipes in heat exchange systems. This kind of thermal flows may be modeled using the unsteady Boussinesq approximation in the Stream function-vorticity formulation.*
Results are obtained with a simple numerical method previously reported for isothermal/natural and mixed convection flows. The numerical method is based on a fixed point iterative process to solve the non-linear elliptic system that results after an appropriate discretization in time.
The iterative process leads us to the solution of uncoupled, well-conditioned and symmetric linear elliptic problems for which very efficient solvers are known to exist regardless of the space discretization.

1 INTRODUCTION

We present a numerical simulation of unsteady plumes for driven thermal high convection dominated flows. The iterative process used in this work, leads us to the solution of uncoupled, well-conditioned and symmetric linear elliptic problems.

The numerical method has been previously reported in [1] for mixed convection and in [2] for natural convection in tilted cavities. This scheme has shown to be robust enough to handle high Rayleigh numbers and different aspect ratios (ratio of the height to the width) of the cavity.

The evolution of the flows we are dealing with in this paper depends mainly on the variation of the parameters. The buoyancy forcing of the flow can be characterized by the Rayleigh number Ra, which in the case of this work, is taken in the range $10^6 \leq Ra \leq 2 * 10^8$. For this range of the Rayleigh number, numerical results are not easy to obtain, since in this case we have a highly convection-dominated thermally-driven problem as can be seen in [3] and [4].

Numerical simulation has been applied to this kind of flows and results with a 2D Direct Numerical Simulation (DNS) have been reported in [5] and [6]. For the validation of our results we are comparing them with those reported in the cited bibliography.

2 MATHEMATICAL MODEL

Let $\Omega \subset R^N$ $(N = 2, 3)$ be the region of a non-steady, viscous, incompressible flow, and Γ its boundary. Under the hypothesis of the Boussinesq approximation, this kind of fluids may be modeled by the following adimensional system:

$$\begin{aligned} \mathbf{u}_t - \nabla^2\mathbf{u} + \nabla p + (\mathbf{u}\cdot\nabla)\mathbf{u} &= \frac{Ra}{Pr}\theta\mathbf{e} \qquad (a) \\ \nabla\cdot\mathbf{u} &= 0 \qquad (b) \\ \theta_t - \frac{1}{Pr}\nabla^2\theta + \mathbf{u}\cdot\nabla\theta &= 0 \qquad (c) \end{aligned} \tag{1}$$

in Ω, $t > 0$; where $\mathbf{u}$, p and θ are the velocity, pressure and temperature of the fluid, respectively, $\mathbf{e}$ is the unitary vector in the gravitational direction. The parameters Ra y Pr are the Rayleigh and the Prandtl number respectively, which are given by: $Ra = \frac{\beta l^3 \kappa g \rho_0^2}{\mu^3 c_p}(T_l - T_0)$, $Pr = \kappa/\mu c_p$, where T_0 and T_1 are reference temperatures, $T_0 < T_1$, which may be the temperatures of the side walls when the region is a rectangular cavity. The adimensional temperature θ is given by $\theta = \frac{T - T_0}{T_1 - T_0}$.

This system must be provided with appropiate initial and boundary conditions:$\mathbf{u}(\mathbf{x}, 0) = \mathbf{u}_0(\mathbf{x})$ and $\theta(\mathbf{x}, 0) = \theta_0(\mathbf{x})$ in Ω; $\mathbf{u} = \mathbf{f}$ and $B\theta = 0$ in Γ, $t \geq 0$, where B is a boundary operator for the temperature and may involve Dirichlet, Neumann and mixed boundary conditions.

Restricting ourselves to a bidimensional region Ω, taking the curl in both sides of equation $(1a)$ and taking into account that:

$$u_1 = \frac{\partial\psi}{\partial y}\,, \quad u_2 = -\frac{\partial\psi}{\partial x}\,, \tag{2}$$

which follows from $(1b)$, with ψ the stream function and $(u_1, u_2) = \mathbf{u}$; the component in the $\mathbf{k} = (0, 0, 1)$ direction, we get the following scalar system:

$$\begin{aligned} \nabla^2\psi \quad\quad\quad\quad &= -\omega \quad (a) \\ \omega_t - \nabla^2\omega + \mathbf{u}\cdot\nabla\omega &= \frac{Ra}{Pr}\frac{\partial\theta}{\partial x} \quad (b) \\ \theta_t - \gamma\nabla^2\theta + \mathbf{u}\cdot\nabla\theta = 0;, &\quad (c) \end{aligned} \tag{3}$$

where $\gamma = 1/Pr$ and ω is the vorticity, which, from $\omega\mathbf{k} = \nabla\times\mathbf{u} = -\nabla^2\psi\mathbf{k}$, gives $(3a)$ and $\omega = \frac{\partial u_2}{\partial x} - \frac{\partial u_1}{\partial y}$ also.

Then, system (3) becomes the Boussinesq approximation in stream function-vorticity variables. The incompressibility condition $(1b)$, by (2), is automatically satisfied and the pressure p has been eliminated.

A translation of the boundary conditions in terms of the velocity primitive variable $\mathbf{u}$ to the $\psi - \omega$ variables has to be performed. Following [7], ψ is a constant function on solid and fixed walls; at the moving wall $y = b$, a constant function for ψ is also obtained, then $\psi = 0$ is chosen in Γ. By Taylor expansion of $(3a)$ on the boundary, with h_x and h_y the space steps, one obtains

$$\begin{aligned} \omega(0,y,t) &= -\frac{1}{2h_x^2}[8\psi(h_x,y,t) - \psi(2h_x,y,t)] + O(h_x^2) \\ \omega(a,y,t) &= -\frac{1}{2h_x^2}[8\psi(a-h_x,y,t) - \psi(a-2h_x,y,t)] + O(h_x^2) \\ \omega(x,0,t) &= -\frac{1}{2h_y^2}[8\psi(x,h_y,t) - \psi(x,2h_y,t)] + O(h_y^2) \\ \omega(x,b,t) &= -\frac{1}{2h_y^2}[8\psi(x,b-h_y,t) - \psi(x,b-2h_y,t)] - \frac{3}{h_y} + O(h_y^2). \end{aligned} \tag{4}$$

.

where h_x and h_y denote the size of the spatial discretization in the x and y directions. It should be observed that the boundary values for ω are given by values in Ω and $t > 0$, still unknown, of the stream function ψ. This problem will be solved using a fixed point iterative process.

3 NUMERICAL METHOD

The time derivatives with respect to ω and θ in (3) are approximated using the following second order approximation:

$$f_t(\mathbf{x}, (n+1)\Delta t) \approx \frac{3f^{n+1} - 4f^n + f^{n-1}}{2\Delta t}, \tag{5}$$

where $n \geq 1$, $\mathbf{x} \epsilon \Omega$, $\Delta t > 0$ is the time step, and $f^r \approx f(\mathbf{x}, r\Delta t)$; at each time level $t = (n+1)\Delta t$ the following semidiscrete system in Ω is obtained , with the corresponding boundary conditions on Γ:

$$\begin{aligned} \nabla^2 \psi^{n+1} &= -\omega^{n+1}, \qquad \psi^{n+1}|_\Gamma = 0, \\ \alpha\omega^{n+1} - \nabla^2\omega^{n+1} + \mathbf{u}^{n+1} \cdot \nabla\omega^{n+1} &= \frac{R_a}{Pr}\frac{\partial\theta^{n+1}}{\partial x} + f_\omega, \qquad \omega^{n+1}|_\Gamma = \omega_{bc}^{n+1}, \\ \alpha\theta^{n+1} - \gamma\nabla^2\theta^{n+1} + \mathbf{u}^{\mathbf{n+1}} \cdot \nabla\theta^{n+1} &= f_\theta, \qquad B\theta^{n+1}|_\Gamma = 0. \end{aligned} \tag{6}$$

where $\alpha = \frac{3}{2\Delta t}$, $f_\omega = \frac{4\omega^n - \omega^{n-1}}{2\Delta t}$, and $f_\theta = \frac{4\theta^n - \theta^{n-1}}{2\Delta t}$; ω_{bc} denotes the boundary condition of ω , B denotes the boundary operator for θ mentioned above, and u_1 and u_2 the components of $\mathbf{u}$ in terms of ψ are given by (2).

Denoting $(\psi^{n+1}, \omega^{n+1}, \theta^{n+1})$ by (ψ, ω, θ) the following non-linear elliptic system is obtained:

$$\begin{aligned} \nabla^2\psi &= -\omega, \qquad \psi|_\Gamma = 0 \qquad (a), \\ \alpha\omega - \nabla^2\omega + \mathbf{u} \cdot \nabla\omega &= \frac{Ra}{Pr}\frac{\partial\theta}{\partial x} + f_\omega, \qquad \omega|_\Gamma = \omega_{bc} \qquad (b), \\ \alpha\theta - \gamma\nabla^2\theta + \mathbf{u} \cdot \nabla\theta &= f_\theta, \qquad B\theta|_\Gamma = 0 \qquad (c). \end{aligned} \tag{7}$$

To obtain $(\omega^1, \theta^1, \psi^1)$ in (6), a first order approximation for the time derivatives may be applied through a subsequence with asmaller time step; a stationary system is then also obtained.

Denoting by

$$\begin{aligned} R_\omega(\omega, \psi) &\equiv \alpha\omega - \nabla^2\omega + \mathbf{u} \cdot \nabla\omega - \frac{Ra}{Pr}\frac{\partial\theta}{\partial x} - f_\omega, \\ R_\theta(\theta, \psi) &\equiv \alpha\theta - \gamma\nabla^2\theta + \mathbf{u} \cdot \nabla\theta - f_\theta. \end{aligned} \tag{8}$$

Then, system (7) is equivalent, in Ω, to:

$$\begin{aligned} \nabla^2\psi &= -\omega, \qquad \psi|_\Gamma = 0, \\ R_\omega(\theta, \psi) &= 0, \qquad \omega|_\Gamma = \omega_{bc} \\ R_\theta(\omega, \psi) &= 0, \qquad B\theta|_\Gamma = 0 \end{aligned} \tag{9}$$

To solve this system at each time level $(n+1)\Delta t$, the following fixed point iterative process is applied in Ω:[8]

With $\{\theta^0, \omega^0\} = \{\theta^n, \omega^n\}$ given, solve "until convergence" on θ and ω

$$\begin{aligned}
\nabla^2\psi^{m+1} &= -\omega^m, \quad \psi^{m+1} = 0 \ \text{ on } \ \Gamma, \\
\theta^{m+1} &= \theta^m - \rho_\theta(\alpha I - \gamma\nabla^2)^{-1}R_\theta(\theta^m, \psi^{m+1}), \\
B\theta^{m+1} &= 0 \ \text{ on } \ \Gamma, \quad \rho_\theta > 0, \\
\omega^{m+1} &= \omega^m - \rho_\omega(\alpha I - \nabla^2)^{-1}R_\omega(\omega^m, \psi^{m+1}), \\
\omega^{m+1} &= \omega_{bc}^{m+1} \ \text{ on } \ \Gamma, \quad \rho_\omega > 0,
\end{aligned} \tag{10}$$

and then take $(\omega^{n+1}, \psi^{n+1}, \theta^{n+1}) = (\omega^{m+1}, \psi^{m+1}, \theta^{m+1})$.

With "until convergence" we mean until two consecutive values of θ and ω, that is, θ^{m+1} and θ^m, and ω^{m+1} and ω^m, differ by less than a certain tolerance, tol, given.

Then, at each iteration, *three* linear elliptic problems associated with the operators: ∇^2, $\alpha I - \gamma\nabla^2$, and $\alpha I - \nabla^2$ have to be solved in Ω. For the discretization of such problems, either finite elements or finite differences may be used, as long as rectangular domains, as in the case of this work, are considered.

4 NUMERICAL RESULTS

Our numerical experiments take place in a rectangular cavity $\Omega = [0,1] \times [0,1]$. The walls of the cavity are solid and fixed. For the temperature, the source in the bottom is taken as a smooth Gaussian hill: $\frac{\partial T}{\partial n} = e^{-F(x-x_0)^2}$, with x_0 the center. The side walls are adiabatic, and on the top wall, zero temperature is prescribed. No-slip boundary conditions for the velocity are imposed on all the walls of the cavity. A translation of the boundary condition in terms of the velocity primitive variable u to the $\psi - \omega$ variables has been performed using (4). The cavity is supposed to be filled with air.

In the following Figures we show the Stream Function (left) and the isotherms (right) for different values of the Rayleigh number.

In Figure 1 we show results for $Ra = 10^6$, at $t = .05$ with $h_x = h_y = 1/256$ and $\Delta t = .00001$. In the graph of the streamline function two vortices in counter flow, but of the same intensity, can be observed. The isotherms, in this case, are symmetric with respect to the source of heat, occupying only part of the cavity.

Increasing the Rayleigh number to 10^7, in Figure 2, we show results at $t = .05$ with $h_x = h_y = 1/256$ and $\Delta t = .00001$. In this case, we can observe just one vortex in the graph of the streamline function with its maximum located at the center of the cavity. Nevertheless, the isotherms begin to show some asymmetry, bending towards the right wall, and presenting a fold at the left top part without filling still the cavity. This indicates that the flow of heat is being transported by the movement of the fluid flow.

Increasing, additionally, the Rayleigh number to $Ra = 10^8$, we show, in Figure 3 results at $t = 0.05$ with $h_x = h_y = 1/256$ and $\Delta t = 0.00001$. We can observe here the restoration of two vortices of counterflow, although one dominates the circulation and the other one is smaller. The isotherms present well-defined asymmetric contours with a plume to the right near the heat source and irregular contours in the top right of the cavity.

In Figure 4 we show results for $Ra = 2 * 10^8$ at $t = 0.01$ with $h_x = h_y = 1/256$ and $\Delta t = 0.00001$. The Figure shows changes to double the Rayleigh number and simulation time given. The numerical method shows to be robust enough to obtain these results. This changes show a growth on the small vortex although the circulation is still being dominated by a dominant vortex. The isotherms present more structure what can be interpreted as a greater influence of its direct buoyancy.

In Figures 5 and 6 an increase in time is considered for the same Rayleigh number. Results are shown at $t = 0.05$ with $h_x = h_y = 1/256$ and $\Delta t = 0.00001$. No significant changes in the flow pattern of the two vortices or in the asymmetric structure of the isotherms are observed.

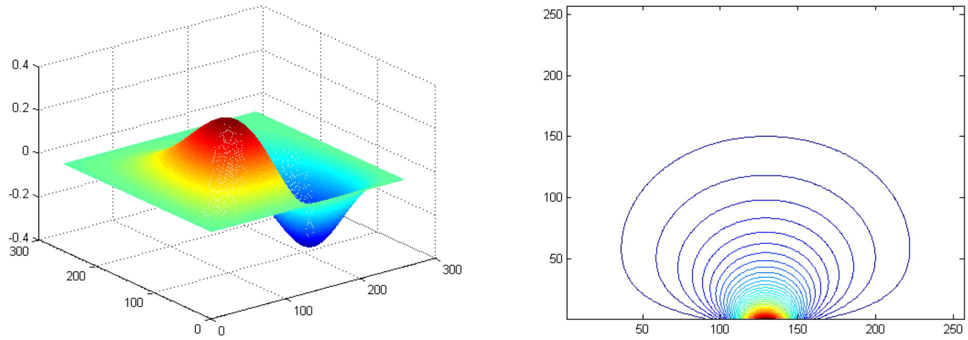

Figure 1: Stream function and isotherms for $Ra = 10^6$, $t = 0.05$, $F = 200$

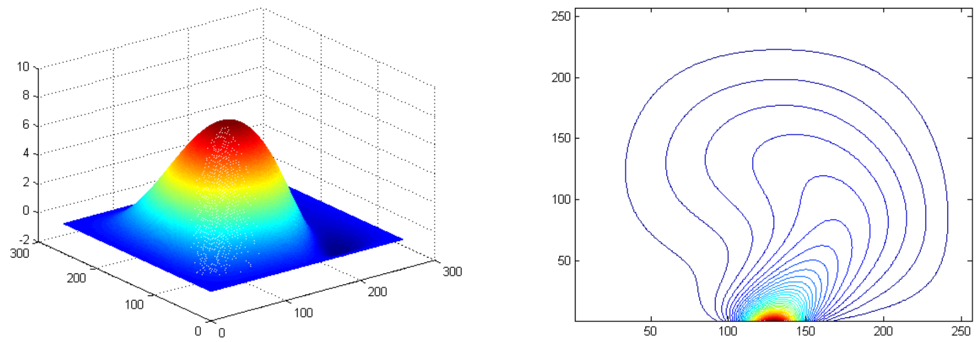

Figure 2: Stream function and isotherms for $Ra = 10^7$, $t = 0.05$, $F = 200$

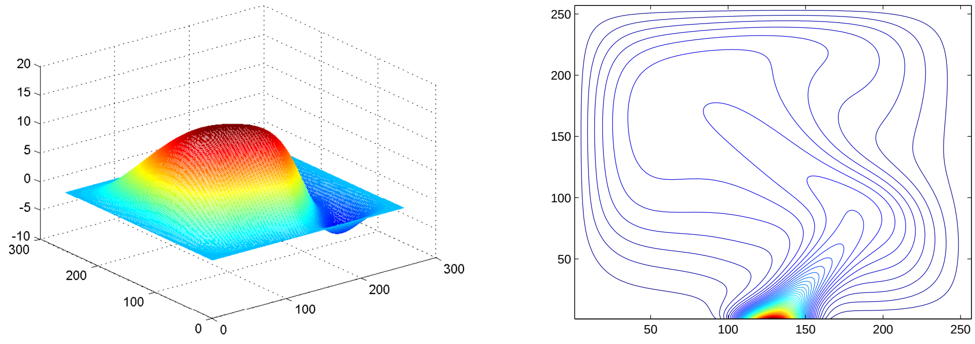

Figure 3: Stream function and isotherms for $Ra = 10^8$, $t = 0.05$, $F = 200$

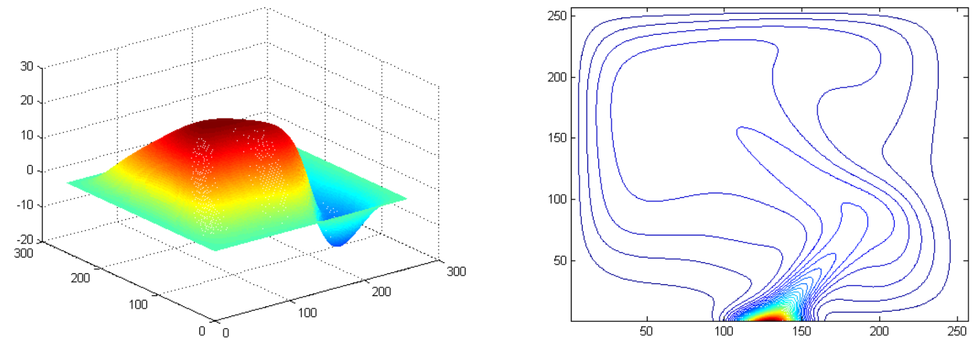

Figure 4: Stream function and isotherms for $Ra = 2 * 10^8$, $t = 0.01$, $F = 200$

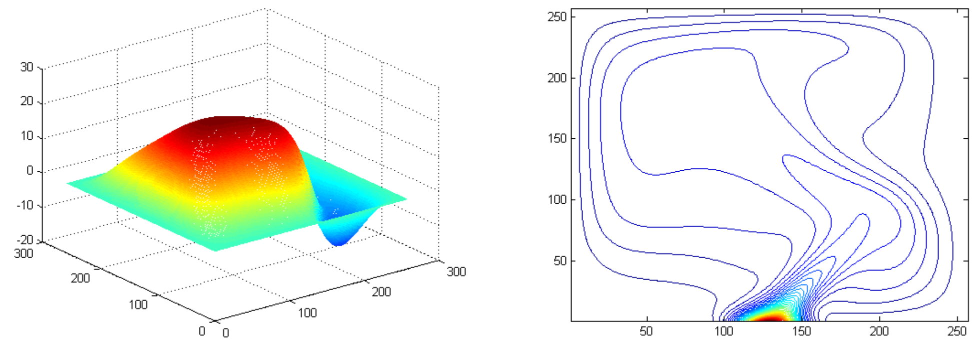

Figure 5: Stream function and isotherms for $Ra = 2 * 10^8$, $t = 0.05$, $F = 200$

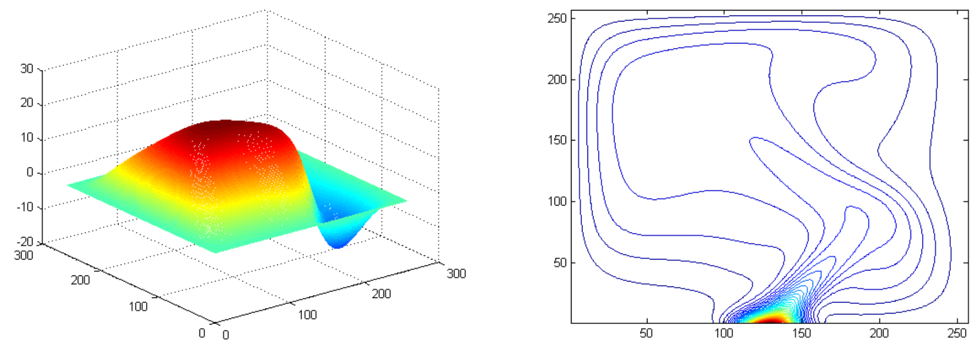

Figure 6: Stream function and isotherms for $Ra = 2 * 10^8$, $t = 0.075$, $F = 200$

5 CONCLUSIONS

The numerical method implemented here lets us distinguish diffusive and convective heat turbulent flow patterns generated in accordance with the increase of Rayleigh number within the cavity. Indeed, to relatively small values of this number the heat diffusion determines the flow profiles (Figure 1) up to $Ra = 10^7$ with only a vortex flow (Figure 2). However, for higher values of this number ($Ra = 10^8$) the isotherm profiles are shifted towards the walls asymmetrically with a dominant convective flow (Figures 3-5) as result of the heat source and the fluid recirculation generated by the turbulent flows within the cavity.

The fixed point iterative process used here has shown to be robust enough to handle very high values of the parameters appearing in the Boussinesq system, such as the Rayleigh number. We are looking forward to improve the method with respect to the time needed for the simulation, since till now, the time needed to solve the numerical systems of equations appearing after the discretization process is very large, especially when working with high Rayleigh numbers and having to arrive to a large value of t (time), since at each iteration in time, a very large system of linear equations has to be solved.

REFERENCES

[1] Nicolás, A. and Bermúdez, B., 2D thermal/isothermal incompressible viscous flows, *Int. J. Numer. Meth. Fluids*,48, pp. 349-366, 2005.

[2] Báez E., Nicolás A., 2D natural convection flows in tilted cavities: porous media and homogeneous fluids, *Int. J. of heat and Mass Transfer*, vol. 49, 4773-4785, 2006.

[3] Minev, P.D., van de Vosse F.,N., Timmermans L. J. P., Rindt, C. C. M., van Steenhoven, A. A., Numerical simulation of buoyant plumes using a spectral element technique, Proceedings of Heat Transfer 94, Advanced Computational Methods in Heat Transfer,(ed. Wrobel, Brebbia and Nowak), Computational Mechanics publications, Southampton,Boston, 147-154, 1994.

[4] Bastiaans, R.G.M., Rindt, C.C.M., van Steenhoven, A.A. and Nieuwstadt, F.T.M., Direct and large eddy simulation of the transition of two and three-dimensional plane plumes in a confined enclosure, Int. Journal of Heat and Mass Transfer 43 2375-2393, 2000.

[5] Desrayaud G., G. Lauriat, Unsteady confined buoyant plumes, J. Fluid Mech 158, 245-268, 1985.

[6] Minev, P.D., van de Vosse F.,N., Timmermans L. J. P., van Steenhoven, A. A., A second order splitting algorithm for thermally-driven flow problems, Int. J. Num. Meth Heat Fluid Flow 6(2), 51-60, 1995.

[7] R. Peyret, T.D. Taylor, Computational Methods for Fluid Flow, Springer-Verlag, NY, 1983.

[8] Nicolas, A., A finite element approach to the Kuramoto-Sivashinski equation, Advances in Numerical Methods, SIAM, 1991.